

## Exploration of below threshold $Z'$ mass and coupling determinations at the NLC

Thomas G. Rizzo

Stanford Linear Accelerator Center, Stanford University, Stanford, California 94309

(Received 11 December 1996)

We examine the capability of the Next Linear Collider to determine the mass as well as the couplings to leptons and  $b$  quarks of a new neutral gauge boson  $Z'$  below direct production threshold. By using simulated data collected at several different values of  $\sqrt{s}$ , we demonstrate how this can be done in a model-independent manner via an anonymous case approach. The importance of beam polarization to the success of this program is discussed. The procedure is shown to be easily extended to the case of top and charm quark couplings. [S0556-2821(97)05109-6]

PACS number(s): 12.60.Cn, 14.70.Pw

### I. INTRODUCTION

While the standard model (SM) is in full agreement with all experimental data [1], it is generally believed that new physics must exist at a scale not far beyond the reach of existing accelerators. Associated with this scale may be a host of new and exotic particles. A new neutral gauge boson  $Z'$  is the most well studied of all exotic particles and is the hallmark signature for extensions of the SM gauge group. Current direct searches for the existence of such particles at the Fermilab Tevatron [2] suggest that their masses must be in excess of 500–700 GeV depending upon their couplings to the SM fermions and their kinematically accessible decay modes. If such a particle is found at future colliders, the next step will be to ascertain its couplings to all of the conventional fermions. In this way, we may hope to identify whether this new particle corresponds to any one of the many  $Z'$ 's proposed in the literature or is something else entirely. At hadron colliders, a rather long list of observables has been proposed over the years to probe these couplings—each with its own limitations [3–5]. It has been shown under idealized conditions, at least within the context of  $E_6$ -inspired models, that the CERN Large Hadron Collider (LHC) ( $\sqrt{s} = 14$  TeV,  $100 \text{ fb}^{-1}$ ) will be able to extract useful information on all of the  $Z'$  couplings for  $M_{Z'}$  below  $\approx 1$ –1.5 TeV. It is *not* clear, however, how much of this program can be carried out using realistic detectors at the LHC [5] and how well it generalizes to other extended gauge models since detailed simulation studies have yet to be performed.

At the Next Linear Collider (NLC), when  $\sqrt{s} < M_{Z'}$  (the most likely scenario for a first generation machine given the Tevatron bounds), a  $Z'$  can only manifest itself indirectly as deviations in, e.g., cross sections and asymmetries from their SM expectations. This is analogous to the observation of the SM  $Z$  at energies reached at the SLAC storage ring PEP, DESY  $e^+e^-$  collider PETRA, and KEK TRISTAN through deviations from the expectations of QED. Fortunately, the list of useful precision measurements that can be performed at the NLC is reasonably long and the expected large beam polarization ( $P$ ) plays an important role—essentially doubling the number of useful observables. In the past, analyses of the ability of the NLC to extract  $Z'$  coupling information

in this situation have taken for granted that the value of  $M_{Z'}$  is already known from elsewhere, e.g., the LHC [6,7]. [In fact, one might argue that if a 1-TeV  $Z'$  is discovered at the LHC, a future lepton linear collider designed to sit on this  $Z'$  must be built and will thus quite easily determine all of the  $Z'$  couplings in analogy to the SLAC Linear Collider (SLC) and CERN  $e^+e^-$  collider LEP.] Here we address the more complex issue of whether it is possible for the NLC to obtain information on couplings of the  $Z'$  if the mass were for some reason *a priori* unknown. In this case, we would not only want to determine couplings, but the  $Z'$  mass as well. We will limit our discussion below to the  $e^+e^-$  channel and ignore the additional information available through  $e^-e^-$  collisions [8].

If the  $Z'$  mass were unknown, it would appear that the traditional NLC  $Z'$  coupling analyses would become problematic. Given a set of data at a fixed value of  $\sqrt{s}$  which shows deviations from the SM, one would not be able to *simultaneously* extract the value of  $M_{Z'}$ , as well as the corresponding couplings. The reason is clear: To leading order in  $s/M_{Z'}^2$ , rescaling all of the couplings and the value of  $M_{Z'}$ , by an overall common factor would leave the observed deviations from the SM invariant. In this approximation, the  $Z'$  exchange appears only as a simple contact interaction. Thus as long as  $\sqrt{s} < M_{Z'}$ , the only potential solution to this problem lies in obtaining data on deviations from the SM at *several*, distinct  $\sqrt{s}$  values and combining them into a single fit. It is clear from the beginning that all of the set of  $\sqrt{s}$  values chosen for this analysis cannot lie too far below the  $Z'$  mass; otherwise, we would always remain in the contact interaction limit. It must be, for at least one of the  $\sqrt{s}$  choices, that subleading terms of relative order  $s/M_{Z'}^2$  are of numerical importance. This suggests that the maximum value of  $\sqrt{s}$  within this set should only be about a factor of 2–3 lower than the  $Z'$  mass.

Here we report on a first pass at this kind of analysis, focusing on observables involving only leptons and/or  $b$  quarks. In performing such an analysis, we need to know how many  $\sqrt{s}$  values are needed. We need to know how we distribute the integrated luminosity ( $\mathcal{L}$ ) to optimize the results. Similarly, we must address whether such an analysis can be performed while maintaining model independence. In this *initial* study we begin to address these and some related

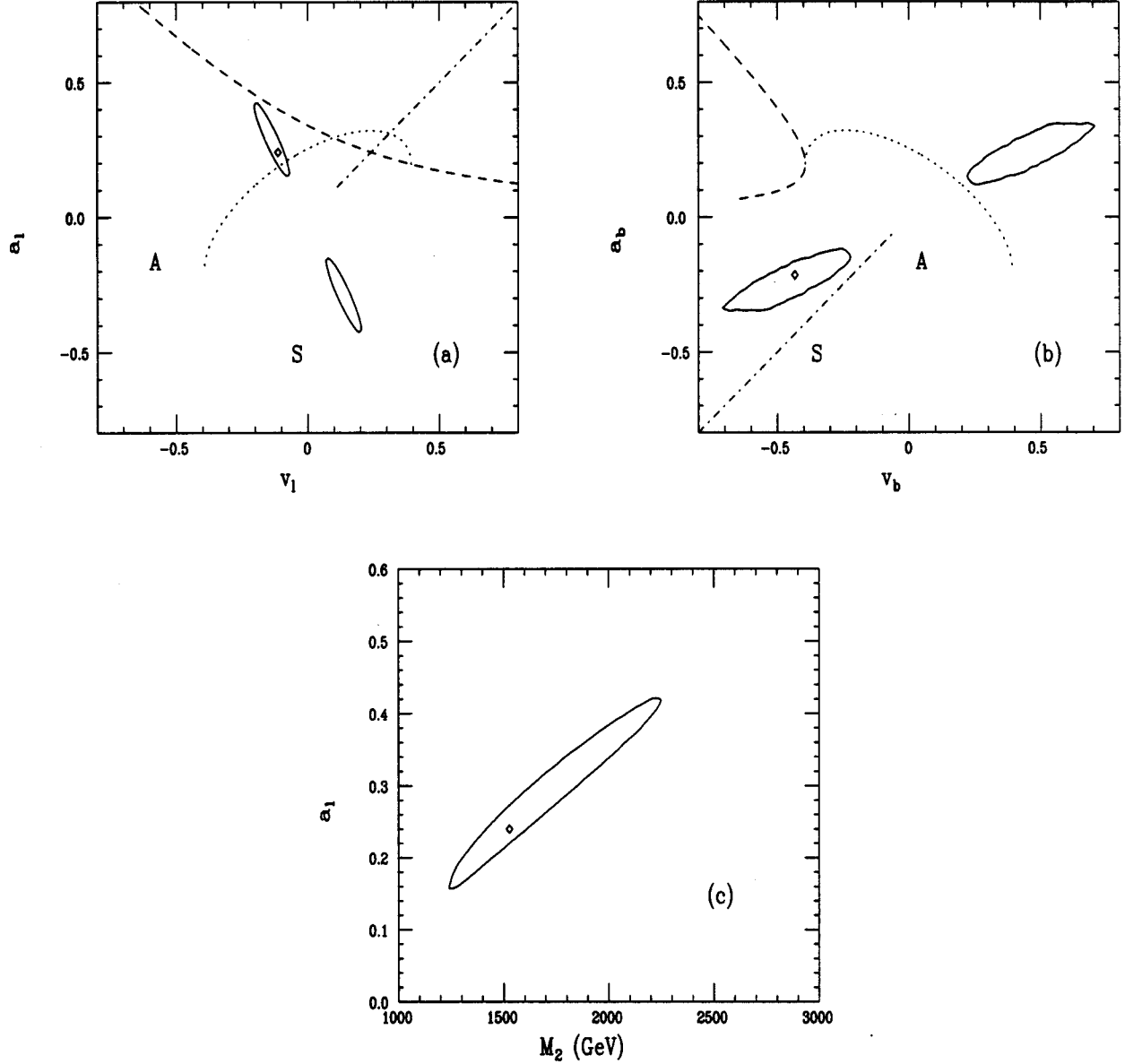


FIG. 1. 95% C.L.-allowed regions for the extracted values of the (a) lepton and (b)  $b$ -quark couplings for the  $Z'$  of case I compared with the predictions of the  $E_6$  model (dotted curves), the left-right model (dashed curves), and the unified model (dash-dotted curves), as well as the sequential SM and alternative LR models (labeled by  $S$  and  $A$ , respectively). (c) Extracted  $Z'$  mass; only the  $a_l > 0$  branch is shown. In all cases the diamond represents the corresponding input values.

issues. It is clear that that there is a lot more to be done before we have the answers to all these questions.

## II. ANALYSIS

In order to proceed with this benchmark study, we will make a number of simplifying assumptions and parameter choices. These can be modified at a later stage to see how they influence our results. (The basic analysis follows that discussed in [9,10].) In this analysis we consider the following ten observables: the total production cross sections for leptons and  $b$  quarks,  $\sigma_{l,b}$ ; the corresponding forward-backward asymmetries  $A_{\text{FB}}^{l,b}$ , the left-right asymmetry obtained from flipping the initial electron beam polarization,  $A_{\text{LR}}^{l,b}$ , and the polarized forward-backward asymmetry

$A_{\text{pol}}^{\text{FB}}(l,b)$ . For  $\tau^+ \tau^-$  final states, we include the average  $\tau$  polarization  $\langle P_\tau \rangle$  as well as the forward-backward asymmetry in the  $\tau$  polarization  $P_\tau^{\text{FB}}$ . Other inputs and assumptions are summarized as follows:

$e, \mu, \tau$  universality

$$P = 90\%, \quad \delta P/P = 0.3\%$$

$$\epsilon_b = 50\%, \quad \Pi_b = 100\%$$

$$\epsilon_{e,\mu,\tau}(\sigma) = 100\%$$

$$\epsilon_\tau(P_\tau) = 50\%$$

initial-state-radiation (ISR)

$$\text{with } \sqrt{s'}/\sqrt{s} > 0.7$$

$$\delta\mathcal{L}/\mathcal{L} = 0.25\%$$

$$|\theta| > 10^\circ$$

neglect  $t$ -channel exchange in

$$e^+ e^- \rightarrow e^+ e^-$$

Of special note on this list of assumptions are (i) a  $b$ -tagging efficiency ( $\epsilon_b$ ) of 50% for a purity ( $\Pi_b$ ) of 100%,

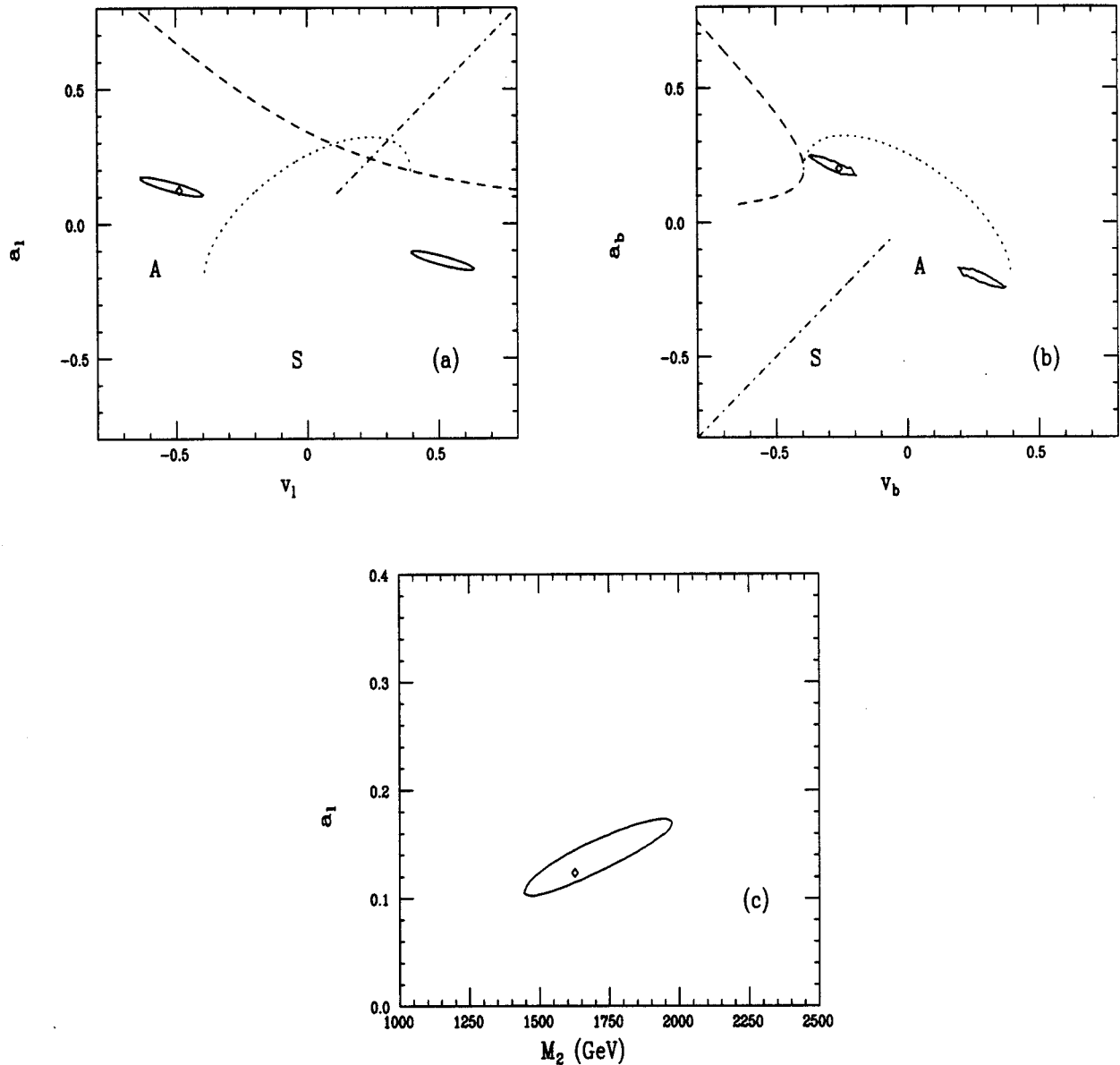


FIG. 2. Same as Fig. 1, but for a different choice of  $Z'$  mass and couplings referred to as case II in the text.

(ii) the efficiency for identifying all leptons is assumed to be 100%, although only 50% of  $\tau$  decays are assumed to be polarization analyzed, (iii) a  $10^\circ$  angle cut has been applied to all final state fermions to mimic the anticipated detector acceptance, (iv) a strong energy cut to remove events with an excess of ISR has been made—this is critical since events with lower effective values of  $\sqrt{s}$  substantially dilute our sensitivity—and (v) it has been assumed that the beam polarization ( $P$ ) and machine luminosity ( $\mathcal{L}$ ) are both well measured. It is important to note that we have *not* included the  $t$ -channel contributions to  $e^+e^- \rightarrow e^+e^-$  in these calculations. This means that we are treating  $e^+e^- \rightarrow e^+e^-$  and  $e^+e^- \rightarrow \mu^+\mu^-$  in an identical fashion. The reason for this is that the usual structure function approach used here to account for ISR does not directly apply when  $u, t$ -channel exchanges are present [11]. The neglect of this  $t$ -channel exchange allows us to simply rescale the  $\mu^+\mu^-$  statistics by a factor of 3 and may be considered an approximation to the

complete result. A recent analysis by Cuypers [11] suggests that this is a good first approximation. If instead this channel is ignored, the statistical errors on the various leptonic observables will increase by only  $\approx 20\%$ . In addition to the above, the final-state multiplicative QED as well as QCD corrections are included to obtain the correct statistics, the  $b$ -quark and  $\tau$  masses have been neglected, and the possibility of any sizable  $Z$ - $Z'$  mixing has also been neglected; this is an excellent approximation for the  $Z'$  mass range of interest to us, given that we are not interested in the  $Z' \rightarrow W^+W^-$  mode. Since our results will generally be statistics limited, the role played by the systematic uncertainties associated with the parameter choices above will generally be rather minimal, especially in the lepton case. Larger systematics should possibly be associated with the  $b$ -quark final states [12], but they have been ignored here for simplicity.

To ensure model independence, the values of the  $Z'$  couplings, i.e.,  $(v, a)_{l,b}$ , as well as  $M_{Z'}$ , are chosen *randomly*

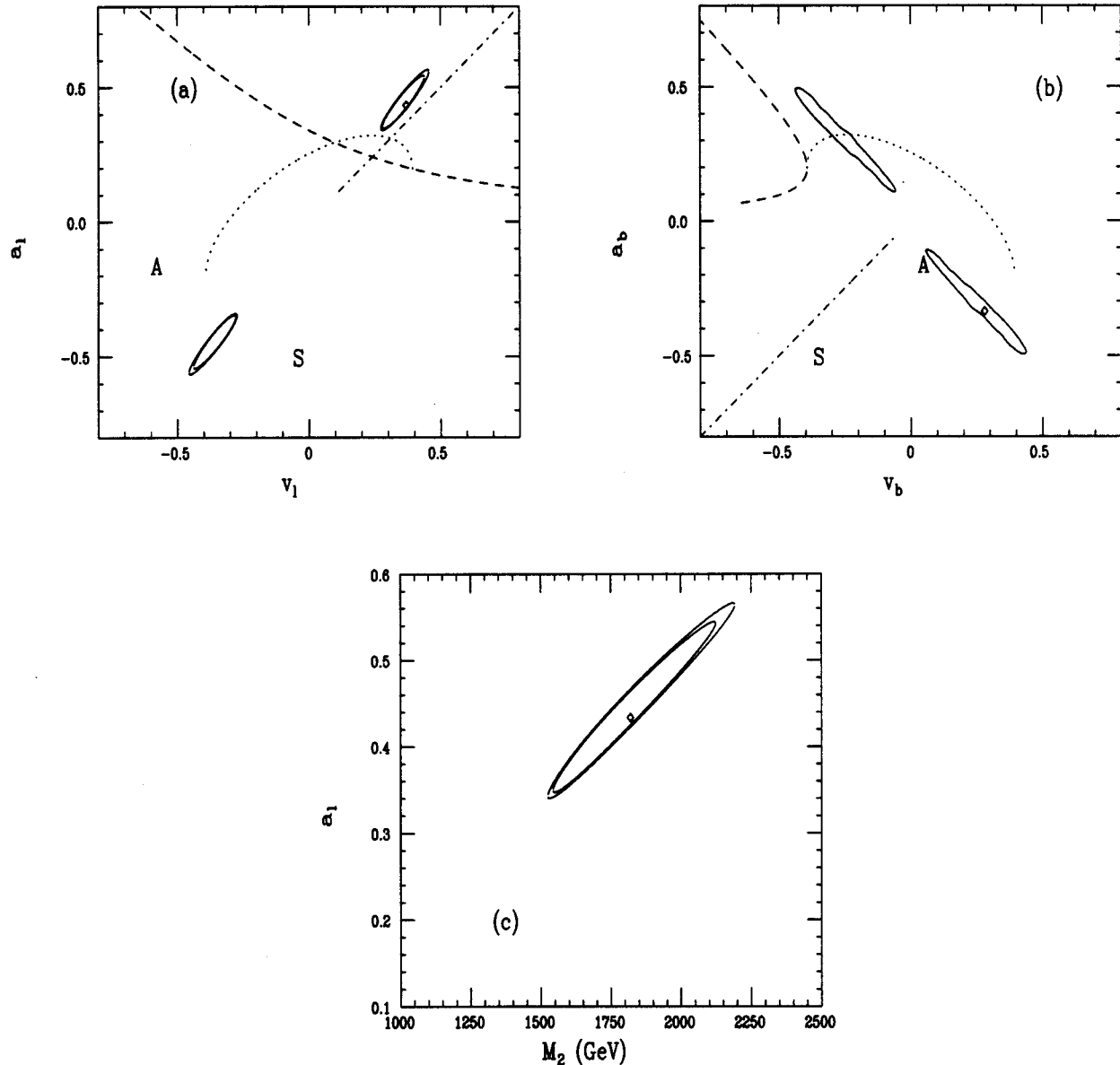


FIG. 3. Same as Fig. 1, but for a third choice of  $Z'$  mass and couplings referred to as case III in the text. The larger (smaller) allowed region in each case corresponds to  $P=80\%$  ( $90\%$ ).

and *anonymously* using a random number generator from rather large ranges representative of a number of extended gauge models. Monte Carlo data representing the above observables are then generated for several different values of  $\sqrt{s}$ . At this point, the values of the mass and couplings are not “known” *a priori*, but will later be compared with what is extracted from the Monte Carlo generated event sample. Following this approach, there is no particular relationship between any of the couplings and there is no dependence upon or relationship to any particular  $Z'$  model. (We chose to normalize our couplings so that for the SM  $Z$ ,  $a_1 = -1/2$ .) Performing this analysis for a wide range of possible mass and coupling choices then shows the power as well as the potential limitations of this technique.

To get an understanding for how this procedure works in general, we will make three representative case studies for the  $Z'$  mass and couplings, labeled here by I, II, and III. There is nothing special about these three choices, and sev-

eral other parameter sets have been analyzed in comparable detail to show that the results that we display below are rather typical. To begin our analysis, let us try choosing three distinct  $\sqrt{s}$  values. Specifically, we generate Monte Carlo “data” at  $\sqrt{s}=0.5, 0.75,$  and  $1$  TeV with associated integrated luminosities of  $70, 100,$  and  $150 \text{ fb}^{-1}$ , respectively. These luminosities are only slightly larger than the typical 1 year values as conventionally quoted [13] and assume a reasonable time evolution of the collider’s center-of-mass energy. Subsequently, we determine the five-dimensional 95% C.L.-allowed region for the mass and couplings from a simultaneous  $\chi^2$  fit to all of the leptonic and  $b$ -quark observables following the input assumptions listed above. This five-dimensional region is then projected into a series of two-dimensional plots, which we now examine in detail. The generation of the data samples and fitting procedures used below required approximately 1500 CPU hours on a DEC ALPHA model 600XMP workstation. Clearly a more de-

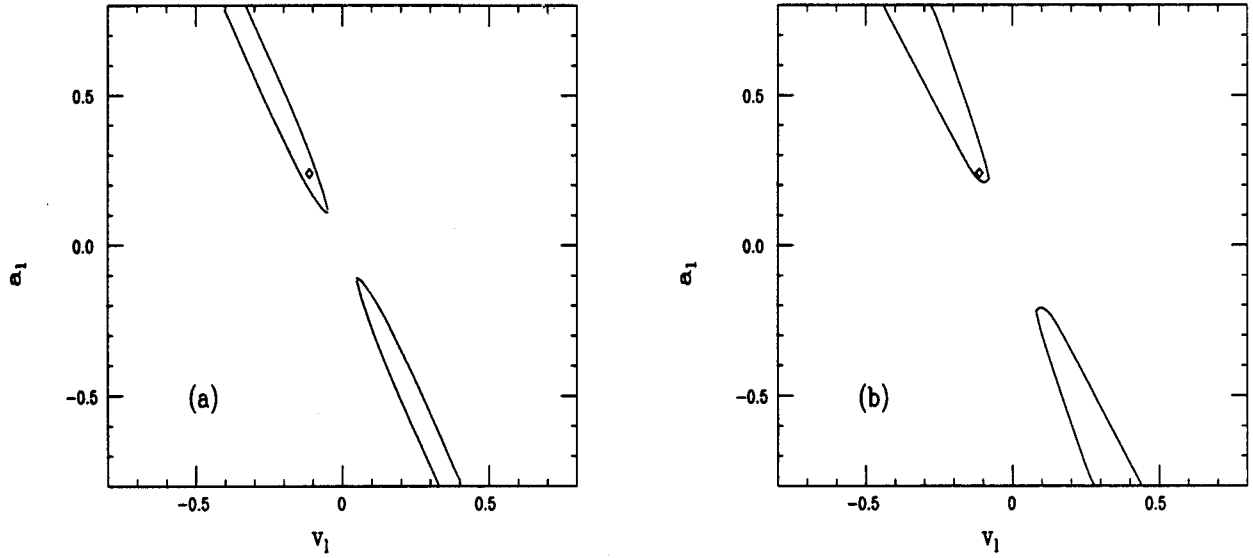


FIG. 4. Failure of the method in case I when data are taken at (a) too few (“two-point” fit) or (b) too many (“six-point” fit) different center-of-mass energies for the same total integrated luminosity as in Figs. 1–3. The luminosities are distributed as discussed in the text.

tailed analysis than the one presented here will require substantially more CPU time.

Figures 1–3 show the results of our analysis for these three case studies compared with the expectations of a number of well-known  $Z'$  models [3]. To be specific we have considered (i) the  $E_6$  effective rank-5 model (ER5M), which predicts a  $Z'$  whose couplings depend on a single parameter  $-\pi/2 \leq \theta \leq \pi/2$ , (ii) the sequential standard model (SSM), wherein the new  $W'$  and  $Z'$  are just heavy versions of the SM particles (of course, this is not a true model in the strict sense, but is commonly used as a guide by experimenters), (iii) the ununified model (UUM), based on the group  $SU(2)_I \times SU(2)_q \times U(1)_Y$ , which has a single free parameter  $0.24 \leq s_\phi \leq 0.99$ , (iv) the left-right symmetric model (LRM), based on the group  $SU(2)_L \times SU(2)_R \times U(1)_{B-L}$ , which also has a free parameter ( $\kappa = g_R/g_L \geq 0.55$ ) of order unity, which is just the ratio of the gauge couplings and, last, and (v) the alternative left-right model (ALRM), based on the same extended group as the LRM, but now arising from  $E_6$ , wherein the fermion assignments are modified in comparison to the LRM due to an ambiguity in how they are embedded in the  $\mathbf{27}$  representation.

By examining these figures, several things are immediately apparent—the most obvious being that two distinct allowed regions are obtained from the fit in all three cases. This ambiguity is twofold and *not* fourfold in that there is a unique choice of  $b$  couplings for a fixed choice of leptonic couplings. (Of course, as we might hope, the input values are seen to lie nicely inside one of them.) This twofold ambiguity occurs due to our inability to make an absolute determination of the overall sign of *one* of the  $Z'$  couplings, e.g.,  $a_1$ . If the sign of  $a_1$  were known, only a single allowed region would appear in Figs. 1–3 for both leptons and  $b$  quarks and a unique coupling determination would thus be obtained. Note that this *same-sign* ambiguity arises in SLC or LEP data for the SM  $Z$  and is only removed through the examination of low-energy neutrino scattering. Second, we see that the leptonic couplings are always somewhat better determined than are those of the  $b$  quark, which is due to the

fact that the leptonic observables involve only leptonic couplings, while those for  $b$  quarks involve both types. In addition, there is more statistical power available in the lepton channels due to the assumption of universality and the fact that the leptonic results employ two additional observables related to the final-state  $\tau$  polarization. The shortage of  $b$ -quark observables, combined with the limited CPU available for the Monte Carlo, is thus responsible for the irregular shape of the allowed region obtained for the  $b$ -quark couplings. If the  $b$ -quark observables had significant systematic errors, these allowed regions would become larger still. Third, we see in particular from Figs. 1(a)–1(b) and 3(a)–3(b) the importance in obtaining coupling information for a number of different fermion species. If only the Fig. 1(a) [3(b)] results were available, one might draw the hasty conclusion that an  $E_6$ -type  $Z'$  had been found. Figure 1(b) [3(a)] clearly shows us that this is not the case. Evidently none of the  $Z'$ 's associated with cases I–III correspond to *any* well-known model. Fourth, we note that changing the beam polarization from 90% to 80% does not appreciably alter our results. Last, as promised, the  $Z'$  mass is determined in all three cases, although with somewhat smaller uncertainties in case II. It is important for the reader to realize that there is nothing special about any of these three particular cases. It is clear from this set of random choices for masses and couplings that this procedure should be viable for  $Z'$  masses up to about 2 TeV for the set of integrated luminosities that we have chosen unless both of the leptonic  $Z'$  couplings are accidentally small, resulting in a reduced sensitivity to the existence of the  $Z'$ .

It is straightforward to extend this analysis to fermion final states other than leptons and the  $b$  quark. The extrapolation to charm is the most obvious in that apart from identification efficiencies and potentially larger systematic errors, there is little difference in performing the five-dimensional  $\chi^2$  fit with either  $b$  or  $c$  since the fermion couplings were randomly chosen. (Of course, we might imagine, however, now doing a more ambitious *seven-dimensional* fit with all of the couplings being allowed to float.) The extension to  $t$

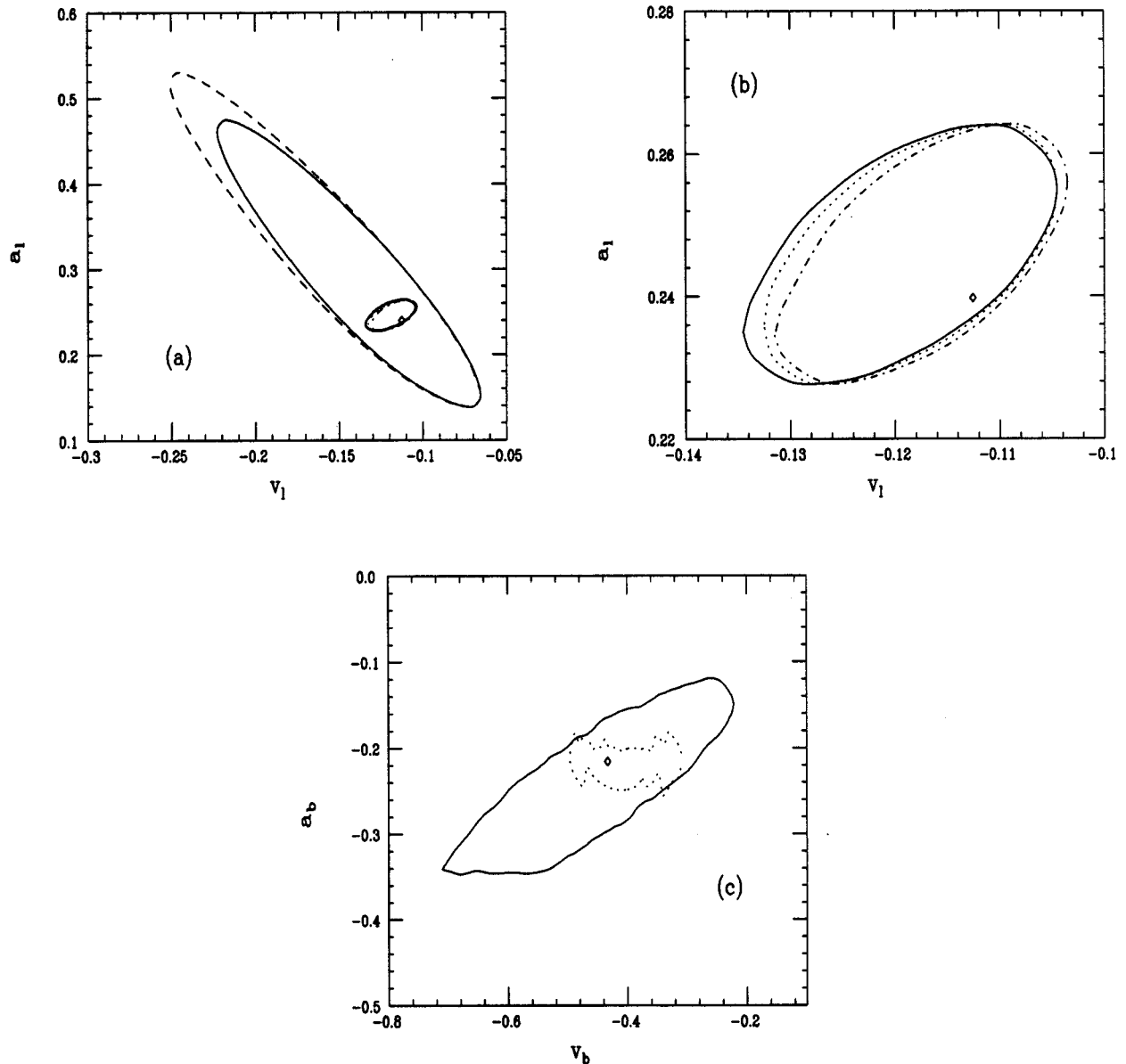


FIG. 5. (a) Expanded lobe (solid curves) from Fig. 1(a); the dashed curve shows the same result, but for  $P=80\%$ . The smaller ovals, expanded in (b), apply when the  $Z'$  mass is known. Here, in (b),  $P=90\%$  (80%) corresponds to the dash-dotted (dotted) curve, while the case of  $P=90\%$  with  $\delta P/P=5\%$  corresponds to the solid curve. (c) Expanded lobe (solid curves) from Fig. 1(b); the dotted curve corresponds to the case when  $M_{Z'}$  is known.

quarks would be less straightforward due to their large mass and rapid decay to  $bW$ . In principle, however, the same set of observables could be constructed for the top quark as was used in the  $b$ -quark analysis above.

Of course, the clever reader must now be asking the question, why did we start off using three different values of  $\sqrt{s}$ —why not two or five? This is a very important issue which we can only begin to address here. Let us return to the mass and couplings of case I and generate Monte Carlo “data” for only two values of  $\sqrt{s}=0.5$  and 1 TeV with luminosities of  $\mathcal{L}=100$  and  $220 \text{ fb}^{-1}$ , respectively, thus keeping the total  $\mathcal{L}$  the same as in the discussion above. Repeating our analysis we then arrive at the “two-point” fit as shown in Fig. 4(a); unlike Fig. 1(a), the allowed region in the leptonic coupling plane does not close and extends out-

ward to ever larger values of  $v_1, a_1$ , we find that a similar result occurs for the  $b$ -quark couplings, which are even more poorly determined. The corresponding  $Z'$  mass contour is also found not to close, again extending outwards to ever larger  $M_{Z'}$  values. We realize immediately that this is just what happens when data at only a single  $\sqrt{s}$  are available. For our fixed  $\mathcal{L}$ , distributed as we have now done, we see that there is not a sufficient lever arm to simultaneously disentangle the  $Z'$  mass and couplings. Of course, the reverse situation can also be just as bad. We now generate Monte Carlo “data” for the case I mass and couplings in 100-GeV steps in  $\sqrt{s}$  over the 0.5–1 TeV interval with the same total  $\mathcal{L}$  as above, but now distributed as 30, 30, 50, 50, 60, and  $100 \text{ fb}^{-1}$ , respectively. We then arrive at the “six-point” fit shown in Fig. 4(b), which suffers from a problem similar to

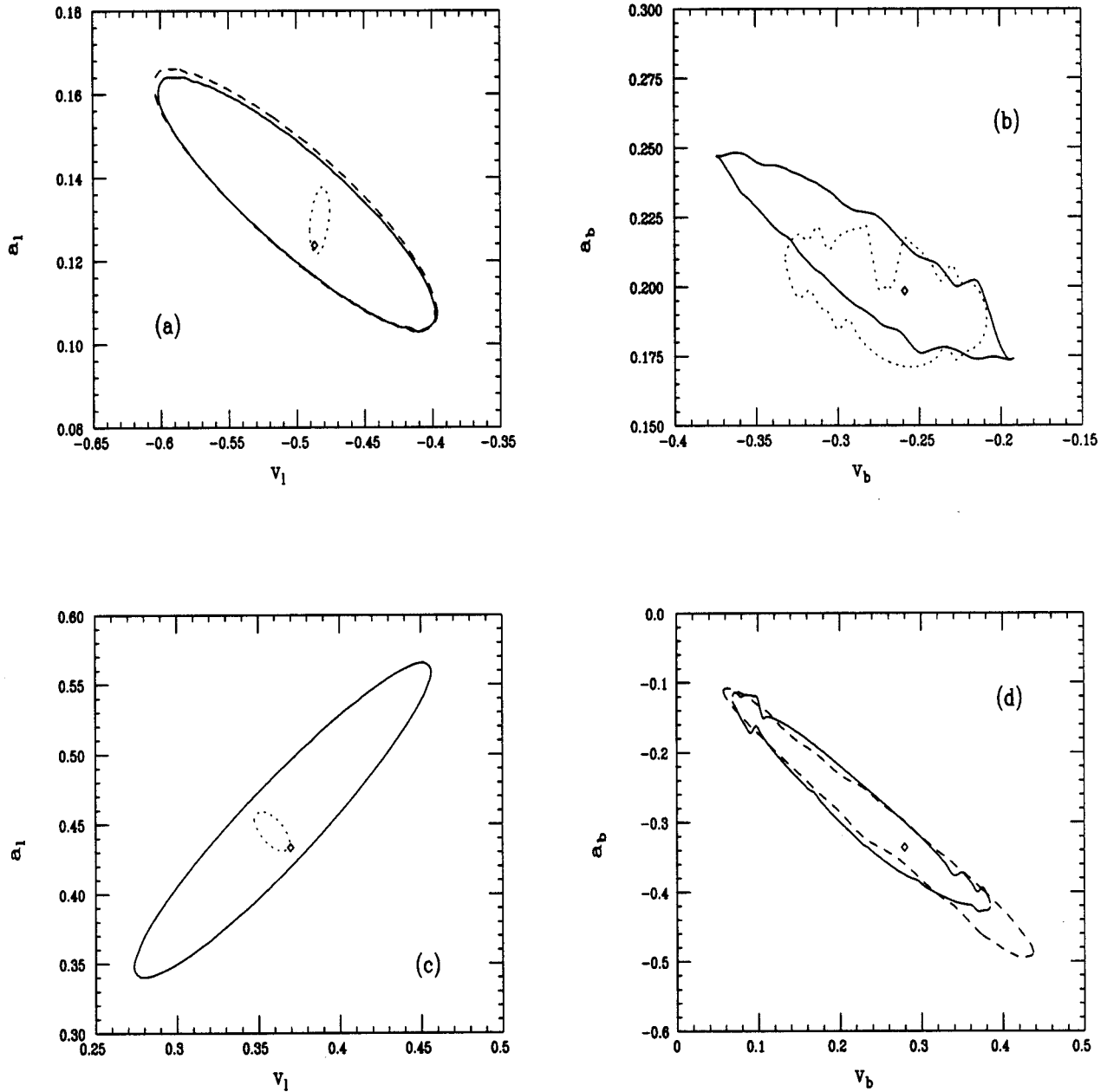


FIG. 6. (a) Expanded lobe (solid curves) from Fig. 2(a); the dashed curve shows the same result but for  $P=80\%$ . The smaller dotted oval, applies when the  $Z'$  mass is known and  $P=90\%$ . (b) Expanded lobe (solid curves) from Fig. 2(b); the dotted curve corresponds to the case when  $M_{Z'}$  is known. (c) and (d) show the corresponding results for case III from Figs. 3(a) and 3(b).

that presented in Fig. 4(a). What has happened now is that we have spread the fixed  $\mathcal{L}$  too thinly over too many points for the analysis to work. These same results are found to hold for all three cases. This brief study indicates that a proper balance is required to simultaneously achieve the desired statistics as well as an effective lever arm to obtain the  $Z'$  mass and couplings. It is important to remember that we have *not* demonstrated that the “two-point” fit will never work. We note only that it fails with our specific fixed luminosity distribution for the masses and couplings associated with cases I–III. It is possible that for “lucky” combinations of masses and couplings a two-point fit will suffice, or it may work if substantially more luminosity is achievable. It is cer-

tainly true that all cases where at least three values of  $\sqrt{s}$  are used will allow simultaneous mass and coupling extraction provided the integrated luminosity is available. Clearly, more work is required to further address these issues.

How do these results change if  $M_{Z'}$  were known or if our input assumptions were modified? In this case we use as additional input in our analysis the value of  $M_{Z'}$ , chosen by the Monte Carlo method and perform four-dimensional  $\chi^2$  fits to the same set of “data.” Let us return to case I and concentrate on the allowed coupling regions corresponding to a choice of negative values of  $v_{l,b}$ ; these are expanded to the solid curves shown in Figs. 5(a) and 5(c). (There will also be a corresponding region where  $v_{l,b}$  are positive, which

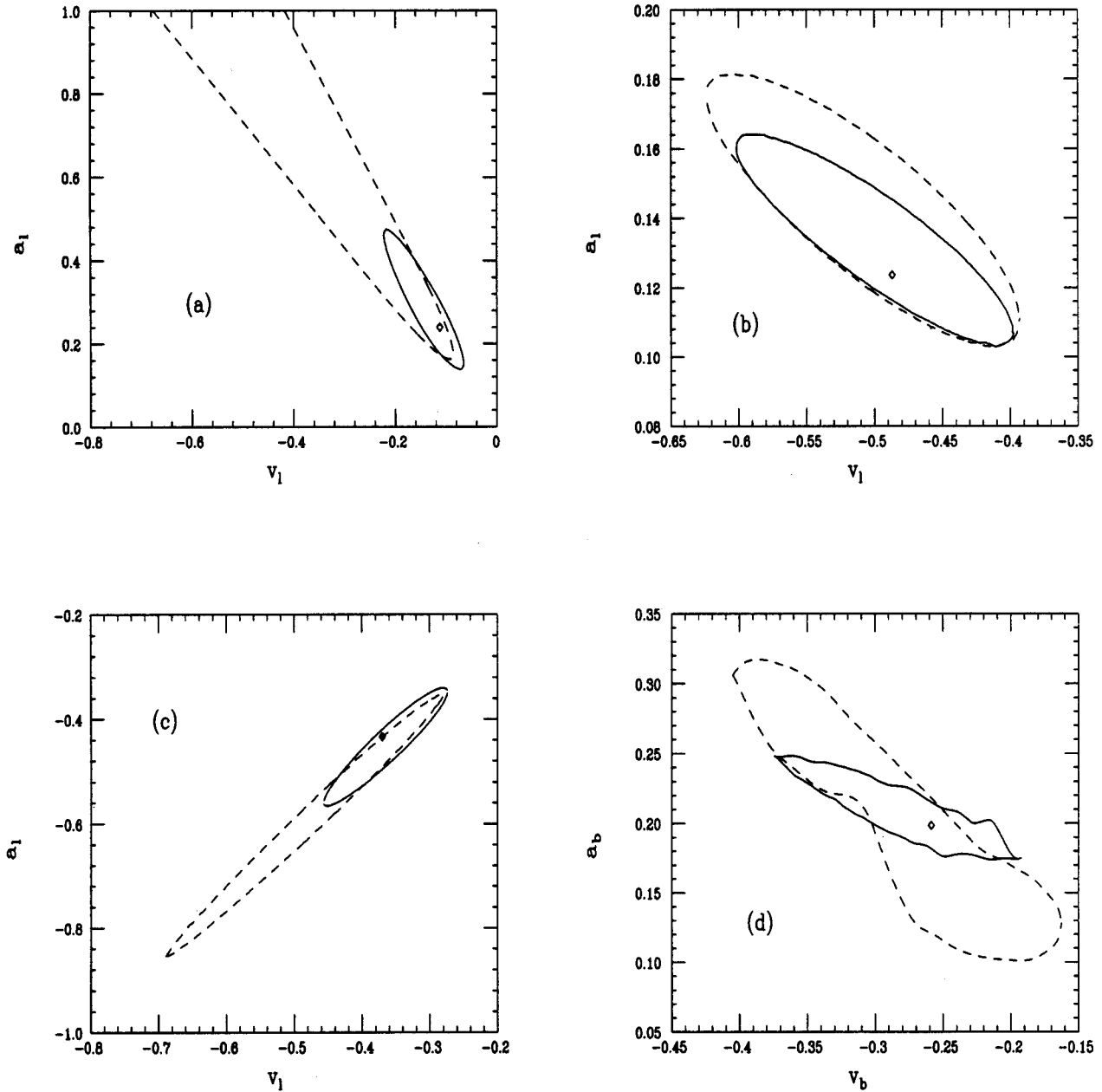


FIG. 7. Comparison of the constraints obtained on the  $Z'$  leptonic couplings in cases I–III, in (a)–(c), respectively, both with (solid curves) and without (dashed curves) observables associated with beam polarization. In (d) are shown the corresponding  $b$ -quark couplings obtained for case II.

we ignore for the moment.) The large dashed curve in Fig. 5(a) corresponds to a reduction of the polarization to 80% with the same relative error as before. While the allowed region expands, the degradation is not severe. If the  $Z'$  mass were known, the “large” ellipses shrink to the small ovals in Fig. 5(a); these are expanded in Fig. 5(b). (Note that the allowed regions shown in this figure correspond to fits to three distinct data samples generated under the three assumptions under consideration.) This is clearly a radical reduction in the size of the allowed region. We see that when the mass is known, varying the polarization or its uncertainty over a reasonable range has very little influence on the resulting size of the allowed regions. From Fig. 5(c) we see that while knowing the  $Z'$  mass somewhat reduces the size

of the allowed region for the  $b$  couplings (the jagged shape of the allowed region and the fact that it is not entirely contained within the corresponding region when  $M_{Z'}$  is known, again being due to limited Monte Carlo statistics), the impact is far less than in the leptonic case for the reasons discussed above. The important point here is that knowing the  $Z'$  mass does not seem to help us a great deal in determining the  $b$ -quark couplings.

Figures 6(a)–6(d) show that case I is not special in that similar results are seen to hold as well for cases II and III. For both of these cases, as in case I, there is an enormous reduction in the size of the allowed region for the leptonic couplings of the  $Z'$ , but the corresponding allowed region for the  $b$  quark shrinks by about only a factor of 2. In case



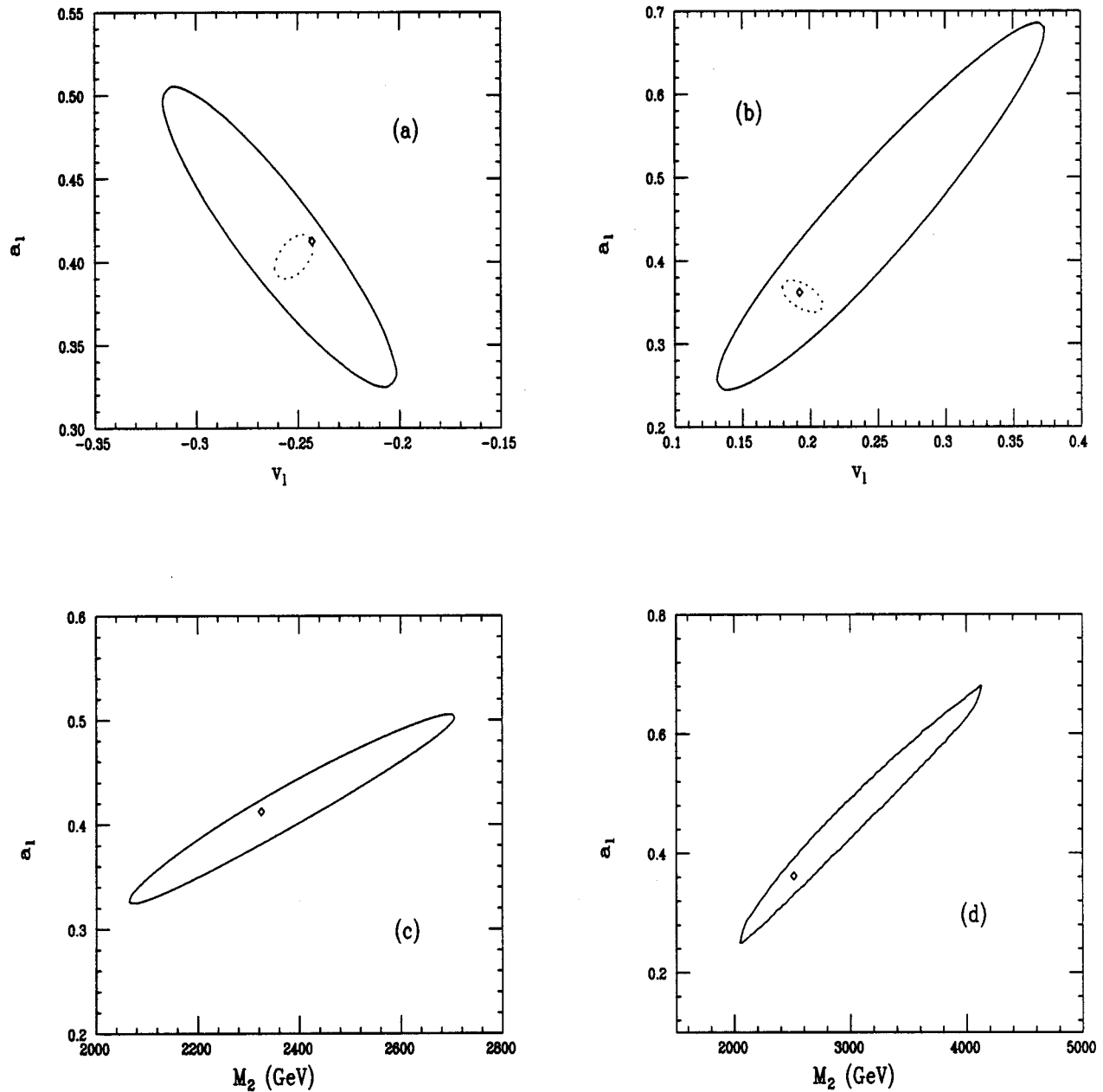


FIG. 8. Lepton coupling determination for  $Z'$ 's with masses of (a) 2.33 TeV and (b) 2.51 TeV when the mass is unknown (solid curves) and known (dotted curves) corresponding to cases IV and V discussed in the text. (c) and (d) are the corresponding mass determinations which result from the five-dimensional  $\chi^2$  fit. These results include an additional  $200 \text{ fb}^{-1}$  of luminosity taken at a center-of-mass energy of 1.5 TeV.

III, there is hardly *any* reduction in the size of the allowed  $b$ -quark coupling region.

In Figs. 5(b) and 6(a) (as well as in some of the later figures below), we will see the curious behavior that the input value is often very close to the boundary of the 95% C.L.-allowed region. If we did not know where the position of the best fit point were or what the  $\chi^2$  contours inside the allowed region looked like, this would give one pause. One finds that the best fit points are *not* generally at the center of the allowed region and lie, in fact, very close to the input values and generally not far from the boundary. For example, in Fig. 5(b) [6(a)] the best fit value for  $v_1$  and  $a_1$  in the case of  $P=90\%$  and  $\delta P/P=0.3\%$  is located at  $(-0.117,$

$0.246)$   $[(-0.483, 0.129)]$  whereas the input values are  $(-0.113, 0.240)$   $[(-0.487, 0.124)]$ . This tells us that the  $\chi^2$  curves are often very highly compressed in the region near the input value since they lie near the edge of the allowed region.

Just how large a role does large beam polarization play in obtaining our results? This becomes a critical issue, especially at higher energies, if our lepton collider is actually a muon collider where we may need to trade off luminosity for high beam polarization [14]. As an extreme case, we repeat the previous analysis of cases I–III without including the observables associated with beam polarization in the fits; luminosities, etc., remain the same as before. The results of

this approach are shown in Figs. 7(a)–7(d). Note that the curves with  $P \neq 0$  do not always completely lie within those where  $P = 0$ ; this is due to the limitations of our Monte Carlo. In case I, shown in Fig. 7(a), the loss of the polarization-dependent observables causes the allowed region in the leptonic coupling plane to open up and no closed region is found. Correspondingly, the  $b$ -quark couplings to the  $Z'$  as well as the  $Z'$  mass are constrained but are no longer localized. Somewhat better results are obtained in cases II and III, shown in Figs. 7(b) and 7(c). For case II, the size of the allowed region essentially doubles in the  $\nu_l$ - $a_l$  plane and triples in the  $\nu_b$ - $a_b$  plane, as shown in Fig. 7(d). The  $M_{Z'}$  constraints are found to relax in a corresponding manner. In case II, while we are hampered by the lack of polarized beams, we are still able to carry out the basic program of coupling extraction and  $Z'$  mass determination—unlike case I. In case III, Fig. 7(c) shows that the leptonic couplings are reasonably constrained without beam polarization, but now neither the  $Z'$  mass nor the  $b$ -quark couplings were found to be constrained. From these considerations we may conclude that beam polarization is of critical importance to this analysis unless the couplings lie in a “lucky” range. It is clear that for *arbitrary* values we will not be able to simultaneously obtain mass and coupling determinations without large beam polarization. We note, however, that this conclusion can soften dramatically if the  $Z'$  mass is already known.

What happens for larger  $Z'$  masses or when data at larger values of  $\sqrt{s}$  becomes available? (As stated above, the “reach” in our coupling determinations was  $\approx 2$  TeV using the “data” at 500, 750, and 1000 GeV.) Let us assume that the “data” from the above three center-of-mass energies are already existent, with the luminosities as given. We now imagine that the NLC increases its center-of-mass energy to  $\sqrt{s} = 1.5$  TeV and collects an additional  $200 \text{ fb}^{-1}$  of integrated luminosity, which corresponds to 1–2 design years. Clearly, for  $Z'$  masses near or below 1.5 TeV, our problems are solved since an on-shell  $Z'$  can now be produced. Thus we shall concern ourselves only with  $Z'$  masses in excess of 2 TeV, inaccessible in the lower energy study above. Figures 8(a)–8(d) show the result of extending our previous procedure—now using four different  $\sqrt{s}$  values, for two distinct choices (IV and V) of the  $Z'$  mass and couplings. These “four-point” results are a combined fit to the data at all four center-of-mass energies. We show the results for both the

general case where  $M_{Z'}$  is unconstrained as well as when it is already determined by other data. (As before, only one of the allowed pair of ellipses resulting from the overall sign ambiguity is shown for simplicity.) Note that the  $Z'$  input masses we have chosen are well in excess of 2 TeV where the LHC may provide only very minimal information on the fermion couplings [3]. Clearly, by using the additional data from a run at  $\sqrt{s} = 1.5$  TeV, this technique can be extended to perform coupling extraction for  $Z'$  masses in excess of 2.5 TeV. The maximum “reach” for the type of coupling analysis we have performed is not yet determined. It seems likely, based on these initial studies, that the extraction of interesting coupling information for  $Z'$  masses in excess of 3 TeV may be possible for a reasonable range of coupling parameters.

### III. OUTLOOK AND CONCLUSIONS

In this paper we have shown that it is possible for the NLC to extract information on the  $Z'$  couplings to leptons and  $b$  quarks even when the  $Z'$  mass is not *a priori* known and, in fact, determine the  $Z'$  mass. This has been demonstrated in a model-independent manner by randomly and anonymously choosing the mass and couplings of the  $Z'$  and demonstrated the power of precision measurements at future linear colliders. The critical step for the success of the analysis is to combine the data available from measurements performed at several different center-of-mass energies. For a reasonable distribution of the luminosities, the specific results we have obtained suggest, but do not prove, that data sets obtained at at least three different energies are necessary for the procedure to be successful. The mass “reach” for this approach is approximately twice the highest center-of-mass energy available. Several questions remain about the optimization of our approach. It is clear that the analysis would benefit by increased Monte Carlo statistics, a better understanding of the systematics associated with  $b$ -quark observables, and a complete analysis of the  $e^+e^- \rightarrow e^+e^-$  channel. These points will be addressed in future work.

### ACKNOWLEDGMENTS

The author would like to thank J. L. Hewett, S. Godfrey, S. Riemann, K. Maeshima, and H. Kagan for discussions related to this work. This work was supported by the U.S. Department of Energy, Contract No. DE-AC03-76SF00515.

- 
- [1] A. Blondel, presented at the 28th International Conference on High Energy Physics, Warsaw, Poland, 1996 (unpublished).  
 [2] CDF Collaboration, M. Pillai *et al.*, Report No. hep-ex/9608006 (unpublished); D0 Collaboration, S. Abachi *et al.*, Phys. Lett. B **385**, 471 (1996).  
 [3] For a complete set of references and a recent review of the physics of new gauge bosons, see M. Cvetič and S. Godfrey, in *Electroweak Symmetry Breaking and Physics Beyond the Standard Model*, edited by T. Barklow, S. Dawson, H. Haber, and J. Seigrist (World Scientific, Singapore 1996).  
 [4] A. Djouadi, presented at the Workshop on Physics and Experi-

- ments with Linear Colliders, Morioka-Appi, Japan, 1995, Report No. hep-ph/9512311 (unpublished).  
 [5] For a very recent summary of  $Z'$  search reaches at various colliders and their capabilities to obtain coupling information, see T. G. Rizzo, Report No. SLAC-PUB-7365, hep-ph/9609248 (unpublished).  
 [6] J. Layssac *et al.*, Montpellier University Report No. PM-96-09, hep-ph/9602327, 1996 (unpublished).  
 [7] A. Leike and S. Riemann, in Proceedings of the Physics with  $e^+e^-$  Linear Colliders Workshop, Annecy-Gan Sasso-Hamburg, 1995, edited by P. Zerwas, Report Nos.

- hep-ph/9604321, hep-ph/9607306 (in press).
- [8] A. Leike, *Z. Phys. C* **62**, 265 (1994); D. Choudhury, F. Cuypers, and A. Leike, *Phys. Lett. B* **325**, 500 (1994); F. Cuypers, *Int. J. Mod. Phys. A* **11**, 1571 (1996); Report No. hep-ph/9611336 (unpublished).
- [9] J. L. Hewett and T. G. Rizzo, *Int. J. Mod. Phys. A* **4**, 4551 (1989); in *Proceedings of the DPF Summer Study on High Energy Physics in the 1990's*, Snowmass, CO, 1988, edited by S. Jensen (World Scientific, Singapore, 1989), p. 235.
- [10] J. L. Hewett and T. G. Rizzo, *Phys. Rep.* **183**, 193 (1989).
- [11] Subsequent to the completion of this work, a first analysis of the  $e^-e^+ \rightarrow e^-e^+$  channel, including the effects of ISR, has been performed by F. Cuypers, Report No. hep-ph/961136 (unpublished). Cuypers has shown that the constraints on the leptonic  $Z'$  couplings in this channel are very similar to what is obtainable from the more conventional  $e^-e^+ \rightarrow \mu^-\mu^+$  channel, implying that the neglect of the  $t$ -channel exchange is a good first approximation to the complete result. However, a more complete analysis of the  $Z'$  leptonic couplings should include these effects.
- [12] The author would like to thank S. Riemann and H. Kagan for discussions on this point.
- [13] See the Zeroth Order Design Report for the Next Linear Collider, "Physics and Technology of the Next Linear Collider," edited by D. Burke and M. Peskin, 1996 (unpublished).
- [14] See "  $\mu^+\mu^-$  Collider Feasibility Study," BNL Report No. BNL-52503, 1996 (unpublished).